

AD-A198 602

DTIC FILE COPY

4

Contract N00014-85-K-0111

**MAGNETIC PROPERTIES  
OF CIV DOPPLER SHIFT PATTERNS**

by  
James A. Klimchuk

CSSA-ASTRO-88-12  
April 1988

DTIC  
ELECTE  
AUG 08 1988  
S H D

**DISTRIBUTION STATEMENT A**

Approved for public release;  
Distribution Unlimited

Contract N00014-85-K-0111

**MAGNETIC PROPERTIES OF  
C IV DOPPLER SHIFT PATTERNS**

James A. Klimchuk<sup>1</sup>

High Altitude Observatory

National Center for Atmospheric Research<sup>2</sup>

April 20, 1988

Submitted to *Solar Physics*

<sup>1</sup> Current address: Center for Space Science and Astrophysics, Stanford University.

<sup>2</sup> The National Center for Atmospheric Research is sponsored by the National Science Foundation.

### Abstract

The relationship between Doppler shift patterns observed in the transition region and magnetic field patterns observed in the photosphere is studied using coaligned pairs of C IV Dopplergrams and Fe I magnetograms. Categories of magnetic features are defined--including neutral lines, unipolar regions, strong field regions, weak field regions, and magnetic boundaries--and from these, magnetic associations are determined for 159  $V_0$  lines separating areas of relative blueshift and redshift observed in and nearby to active regions. The cases are subdivided on the basis of whether blueshifts or redshifts are observed on the side of the  $V_0$  line nearest the limb.

Two of the main results are that  $V_0$  lines associated with neutral lines tend to have limbward blueshifts, while  $V_0$  lines associated with unipolar regions tend to have limbward redshifts. These and other results provide supportive evidence for the active region model proposed recently by Klimchuk, in which relative redshifts occur where strong vertical fields penetrate the surface, and relative blueshifts occur where these same fields have spread out to become horizontal. It is likely that the relative blueshifts correspond to absolute Doppler shifts of very small amplitude, possibly even redshifts.



Accession For	
NTIS GRA&I	<input checked="" type="checkbox"/>
DTIC TAB	<input type="checkbox"/>
Unannounced	<input type="checkbox"/>
Justification	
By <i>per letter</i>	
Distribution/	
Availability Codes	
Dist	Avail and/or Special
<i>A-1</i>	

## 1. Introduction

One of the many interesting results to come from the *Solar Maximum Mission* was the discovery that C IV Doppler shifts are organized into well-defined patterns within active regions. Athay *et al.* (1982, 1983b) were the first to study these patterns and noted that they resemble magnetic polarity patterns seen in photospheric magnetograms. It was shown that many  $V_0$  lines, which are the lines of demarcation between adjacent areas of redshift and blueshift, correspond both in shape and approximate location with magnetic neutral lines. Only about half of the  $V_0$  lines could be identified with neutral lines, however.

In a later study, we also examined the relationship between Doppler shift and magnetic field patterns (Klimchuk, 1987; hereafter Paper I). We used magnetogram images better suited for distinguishing field strength and found that redshifts tend to occur where the field is strong ( $> 100$  G) and blueshifts tend to occur where the field is weak ( $< 100$  G). Thus, many  $V_0$  lines coincide approximately with the boundaries between strong and weak field. It was also noted that  $V_0$  lines can occasionally be observed well inside regions of weak field.

It became apparent that a more detailed and systematic study of the relationship between C IV Doppler shift patterns and photospheric magnetic field patterns was needed. In this paper we report on the results of such a study. Our approach has been to identify and classify the different magnetic features with which  $V_0$  lines are observed to coincide. Since C IV emission originates within  $2\text{--}4 \times 10^3$  km of the photosphere (Klimchuk, 1987), the  $V_0$  lines and magnetic features must

be nearly vertically aligned (although projection effects could be important near the limb; see Athay and Klimchuk, 1987).

We have concerned ourselves with both the polarity and the strength of the field, and we have paid attention to the redshift/blueshift orientation of the  $V_0$  lines with respect to the solar limb. That is, we distinguish between  $V_0$  lines in which redshifts occur on the side nearest the limb and  $V_0$  lines in which blueshifts occur on the side nearest the limb. Athay *et al.* (1982, 1983b) found evidence for a systematic trend in this regard, although as we will see, the trend they identified was incorrect.

In Paper I we showed that the magnetic field vector is mainly vertical within strong field regions, but mainly horizontal within weak field regions (see also Malherbe *et al.*, 1987). This led us to propose a simple model in which the vertical fields diverge very rapidly with height to become essentially horizontal in low-lying surrounding areas. One important consequence of this model is that  $V_0$  lines should have a preferred Doppler shift orientation, depending on whether they overlie a magnetic neutral line or a unipolar region. This provides a useful test of the model and has been an additional motivation for this study.

## 2. Observations and Data Reduction

Since the Dopplergram and magnetogram data used here were described in detail in Paper I, we now provide only a brief summary. The Dopplergram observations were made in the 1548 Å resonance line of C IV by the Ultraviolet Spectrometer and Polarimeter (UVSP) onboard the *Solar Maximum Mission* spacecraft. They indicate approximate Doppler shifts at a temperature of roughly  $10^5$  K. No absolute

wavelength reference was available on UVSP, and it is customary to normalize the Dopplergrams such that the intensity-weighted average Doppler shift vanishes within each image. This does not generally result in an absolute calibration, however (Klimchuk, 1986). The images are 4' on a side and have a spatial resolution of 3". Examples are given in the upper-left frames of Figures 1-3. The magnitudes of the Doppler shifts are typically between 5 and 10 km s<sup>-1</sup>.

The Kitt Peak magnetogram observations were made in the 8688 Å line of Fe I and indicate average line-of-sight field strengths within a 500 km thick layer of the middle to upper photosphere, just below the temperature minimum (Jones and Giovanelli, 1982). The spatial resolution varies with atmospheric seeing, but is nominally around 2".

Our analysis is divided into two parts, using two different sets of magnetogram images. The first set consists of 97 full disk images which were readily available at the beginning of the study. These are general purpose magnetograms which display field strength in a highly nonlinear way so that both weak and strong fields can be seen together in a single image. This makes them very useful for determining the polarities of all but the weakest fields, but they are not well-suited for distinguishing between fields of differing strengths.

For this reason we have obtained a second set of images, consisting of smaller 4' x 4' rasters extracted from the full disk data using the IPPS data processing system at NOAO. Included in this set are magnetic contour plots, linear magnetogram plots, and Fe I "wing spectroheliograms." The latter are made by summing instead of differencing the left and right circular polarization signals. Examples of extracted images are also given in Figures 1-3: in the lower-right

panels are contour plots, showing  $\pm 100$  G contours filled-in black or white depending on the magnetic polarity; in the upper-right are linear magnetogram plots, which is largely saturated and included to show the weak fields; and in the lower-left are Fe I wing spectroheliograms. The spectroheliograms mimic white light observations quite closely and are useful for identifying sunspots. The complete data set consists of 30 of each of these images.

In order to make a detailed comparison of the Dopplergram and magnetogram images it is necessary that they be very accurately coaligned. This, in turn, requires that the images be corrected for the relative distortions caused by solar rotation during the time lapses between observations. As in Paper I, we make these corrections on the computer by artificially rotating the Dopplergrams forward or backward in time to appear as if they had been observed concurrently with the magnetograms. We assume the differential rotation rate of Howard and Harvey (1970), and we take into account the variable tilt of the solar rotation axis out of the plane-of-the-sky (the solar B-angle). Rotated Dopplergrams are then aligned with the magnetograms to an accuracy of usually better than 5" (see Paper I for details). For the results presented here, we include only those cases where the coalignment is accurate to at least 6" at the 70 % confidence level.

### 3. Analysis

#### 3.1. Magnetic Classifications

$V_0$  lines coincide with a variety of different magnetic features, and it is useful to group these features into well-defined classes. We consider two separate, but related, classification systems.

As mentioned above, the full disk magnetograms are only useful for determining magnetic polarities. We therefore define two main classes of magnetic feature for that data set: *unipolar regions* and *magnetic neutral lines*. A unipolar region contains line-of-sight fields of a single polarity, while a neutral line is a line of polarity reversal. Neutral lines thus separate adjacent unipolar regions of opposite polarity.

It is important to remember that the observed line-of-sight polarity does not necessarily correspond with the polarity of the flux through the solar surface. If the field is inclined to the vertical, then the polarity that is observed will depend upon the feature's location on the disk. For steady-state magnetic fields, the polarity of a feature may be seen to reverse as the feature rotates across the disk. This is, in fact, a commonly observed property of many solar fields (Paper I).

For the extracted magnetogram images we are able to define additional categories based on the strength of the field. We include *strong field regions*, *weak field regions*, *magnetic boundaries*, and *strong field neutral lines*. Strong field regions and weak field regions have field strengths of greater than and less than 100 G, respectively. In addition, we require that strong field regions be unipolar. Magnetic boundaries are the boundaries between adjacent strong and weak field regions; the two regions can have equal or opposite polarity. And finally, strong field neutral lines are a special class of neutral line formed by opposite polarity strong field regions whose separation is less than 3". (We must allow a finite separation because the field strength is always less than 100 G in the immediate vicinity of neutral lines.)



We adopt a level of 100 G to distinguish between strong and weak fields, but in most instances the choice is not critical. Gradients in the field tend to be steep near 100 G contours, so that contours at 50 and 150 G are usually very similar. The separation of these contours is typically less than a few arcseconds.

Figure 4 shows schematic drawings of the different magnetic features we have defined. It is clear that the full disk and extracted image classifications are complementary, not mutually exclusive. For example, a magnetic boundary can occur either at a neutral line, as in (b), or within a unipolar region, as in (d). Similarly, a weak field region can be unipolar or it can contain a neutral line.

In addition to these magnetic features, we consider one further category consisting of sunspots. It is not necessary to include this category, since sunspots can always be placed into one of the other categories, but sunspots tend to have their own peculiar Doppler shift and magnetic properties, so to avoid confusion we treat them separately.

### 3.2. Magnetic Associations

We restrict our present analysis to  $V_0$  lines that are at least 75" long and reasonably well-defined along their entire length. Portions of some  $V_0$  lines are not well-defined either because the data are noisy or because the gradient in the Doppler shift is so shallow that the  $V_0$  line is, effectively, a  $V_0$  band of finite width (see Paper I). Figures 1-3 show thirteen of the  $V_0$  lines which are included in our results.

A  $V_0$  line is said to be unambiguously associated with a magnetic feature if the two coincide to within the following tolerances. For neutral lines and magnetic boundaries we require that at least 75 % of

the  $V_0$  line be closer than 6" from the magnetic feature. For unipolar, weak field, and strong field regions we require that at least 75 % of the  $V_0$  line be more than 6" inside the perimeter of the region. A similar criterion is used for sunspots, where we take the perimeter of the sunspot to be the outer edge of the penumbra. When none of these strict conditions is met, the association is deemed to be ambiguous.

All  $V_0$  lines can, in principle, be assigned at least two magnetic associations--one from the full disk classification and one from the extracted image classification. In addition, some  $V_0$  lines are found to be associated with more than one magnetic feature of the same classification (full disk or extracted image). We treat the different segments as separate  $V_0$  lines as long as they individually satisfy the necessary requirements, including the 75" length requirement. Many times sunspots are an inconspicuous part of a larger magnetic feature, such as a strong field region or a neutral line seen near the limb, and we take the primary association to be with the larger feature as long as a majority of the  $V_0$  line is independent of any spots.

The magnetic associations of the numbered  $V_0$  lines in Figures 1-3 are listed in Table I. Both the full disk and extracted image classifications are given. We chose to present these three rasters in particular because of the great variety of magnetic associations that are represented; of all the possible combinations of full disk and extracted image associations, only the unipolar region/strong field region combination is not included. It is quite rare, however, occurring only once in the entire data set.

#### 4. Results

Using the full disk magnetograms we were able to determine magnetic associations for 159  $V_0$  lines observed in and around 34 different active regions. Approximately half of these  $V_0$  lines were also given associations on the basis of the more limited extracted images. Results for the two data sets are given separately in Tables II and III. Total numbers of cases in each class of feature are indicated in the bottom row. Other rows indicate the breakdown on the basis of whether redshifts or blueshifts are observed on the side of the  $V_0$  line nearest the limb. For  $V_0$  lines that are aligned roughly perpendicular to the limb this is not meaningful, and we list them under the separate heading of "neither."

The grand total of cases in Table II is greater than 159 because some  $V_0$  lines were observed repeatedly. However, no  $V_0$  line is counted more than four times--once near the limb ( $\sin\theta > 0.7$ ) and once near disk center ( $\sin\theta < 0.7$ ) in each the eastern and western hemispheres. There are only 22 repeat cases in all, so they have little effect on the overall statistics.

##### 4.1. Full Disk Magnetogram Classification

The unambiguous associations in Table II are divided fairly evenly between unipolar regions and neutral lines; differences are well within the statistical noise. Only a small fraction of the  $V_0$  lines are associated primarily with sunspots. Roughly 40 % of all the cases are ambiguous.

A striking trend in Table II is for the  $V_0$  lines associated with unipolar regions to be preferentially redshifted on their limb side, and

for  $V_0$  lines associated with neutral lines to be preferentially blueshifted. This result applies equally to the eastern and western hemispheres. Sunspot  $V_0$  lines also show a bias for limbward blueshifts, but the trend is considerably milder.

Our result for sunspots agrees well with that found earlier by Athay *et al.* (1982, 1983a). It was originally interpreted as evidence for a reverse Evershed inflow. Our result for neutral lines is not in agreement with the earlier result of Athay *et al.* (1982, 1983b), however. Those authors associated neutral lines primarily with  $V_0$  lines having limbward redshifts, rather than limbward blueshifts.

We can trace this discrepancy to the following two causes: (1) Dopplergram and magnetogram images were only approximately coaligned in the earlier study; and (2)  $V_0$  lines do not appear equally prominent in Dopplergrams.  $V_0$  lines across which the Doppler shift gradient is steep are more distinctive than are  $V_0$  lines across which the gradient is shallow (see Paper I). In most situations, two  $V_0$  lines are present for every neutral line, and it was incorrectly assumed that the more prominent  $V_0$  line of the pair should be identified with the neutral line. The current study shows that the less prominent  $V_0$  line usually coincides with the neutral line, and the more prominent  $V_0$  line lies nearby in a region of unipolar field. Of 65  $V_0$  lines having Doppler shift gradients in excess of  $2 \text{ km s}^{-1} \text{ arcsec}^{-1}$ , roughly four times as many are associated with unipolar regions as with neutral lines.

#### 4.2. Extracted Image Classification

Most of the unambiguous associations in Table III are divided evenly between magnetic boundaries and weak field regions. There is only one example each of a strong field region and strong field neutral line association. As in Table II, nearly half of the associations are ambiguous by our strict criteria.

Weak field  $V_0$  lines have limbward redshifts approximately twice as often as they have limbward blueshifts. Magnetic boundary  $V_0$  lines are just as likely to have limbward blueshifts as limbward redshifts, on the other hand. This is an important result. Upon examining the data further we find that, without exception, the strong field side of the boundary is redshifted and the weak field side of the boundary is blueshifted. Since there is no statistically preferred orientation of magnetic boundaries, there is no statistically preferred orientation of the associated  $V_0$  lines: limbward blueshifts are just as common as limbward redshifts.

The strong field region and strong field neutral line cases have limbward redshifts and blueshifts, respectively, but it is impossible to know if they represent trends. The sunspot cases are of course preferentially blueshifted. It is interesting that the ambiguous cases show no bias for a particular Doppler shift, both in Table II and Table III. This gives us confidence that there are no systematic errors in our analysis.

To complete our study, we further divided the cases in Tables II and III into subgroups. First, we discriminated between observations made near the limb and observations made near disk center. The only

significant difference here is that weak field associations are relatively more common near the limb. This is probably an observational selection effect resulting from the increased ratio of quiet Sun area to active region area in the limb rasters.

Second, we discriminated between Dopplergrams made with the wide exit slit pair on UVSP and Dopplergrams made with the narrow exit slit pair (see Paper I). There are no appreciable differences at all, indicating that the different alignment procedures used for these two types are equally accurate.

## 5. Summary and Discussion

The main results from our study using the extracted magnetogram images can be summarized as follows. Major  $V_0$  lines tend to occur either at the boundaries between *strong* and *weak* field or well within areas of uniformly weak field, but rarely do they occur within areas of uniformly strong field (sunspots excepted). Moreover, when a  $V_0$  line occurs at a magnetic boundary, the strong field side of the boundary is always redshifted and the weak field side of the boundary is always blueshifted.

These results apply strictly to  $V_0$  lines; however, important correlations of the larger-scale Doppler shift and magnetic field patterns are implied. First, since  $V_0$  lines are uncommon within strong field regions, those regions must tend to be everywhere redshifted. This agrees well with the general correlations that were discussed in Paper I.

Second, weak field regions must tend to be blueshifted, but they may also include extended areas of redshift. Apparently strong field

redshifts give way to blueshifts at magnetic boundaries, but the redshifts appear again at some further removed location from the active region. Such behavior is evident in Figure 2 ( $V_0$  line #4) and Figure 3 ( $V_0$  lines #2 and #6), and can also be seen in Figure 3 of Paper I. As noted in Paper I, another situation can arise occasionally in which the redshifts of a strong field region extend well beyond the magnetic boundary into the surrounding region of weak field. This produces a  $V_0$  line with an opposite Doppler shift orientation to that above.

The main results from our study using the full disk magnetograms are that  $V_0$  lines occur equally frequently at neutral lines and within regions of unipolar field, and furthermore that the limbward side of the  $V_0$  lines is blueshifted in the case of neutral lines and redshifted in the case of unipolar regions. These results are independent of the field strength and apply both to magnetic boundaries and to weak field regions.

We can understand these results in the context of the simple model proposed in Paper I. In that model, active region fields penetrate the surface in a nearly vertical fashion within strong field regions, and they diverge very rapidly with height to become essentially horizontal in the upper photosphere and chromosphere of the adjacent weak field regions. The basic topology is shown schematically in Figure 5, where arrows indicate the direction of the magnetic field. Since active regions are bipolar in nature, this drawing represents only one-half of the complete active region.

We consider two separate views of this field--one corresponding to an eastern hemisphere observation and the other corresponding to a western hemisphere observation. "R" and "B" designations indicate the

redshifts and blueshifts that are observed in strong field regions and weak field regions, respectively. A pair of  $V_0$  lines are formed at the magnetic boundaries on either side of the strong field region.

Let us now consider the line-of-sight magnetic polarities that would be observed with the view from the upper-left. The vertical fields of the strong field region are directed toward the observer and are therefore positive. So, too, are the horizontal fields of the weak field region to the left. The horizontal fields of the weak field region to the right are directed away from the observer, on the other hand, and would therefore be observed as negative. Clearly, a neutral line will appear at the rightmost  $V_0$  line. The leftmost  $V_0$  line will be seen to lie within an area of positive unipolar field.

The situation is quite different for the opposing view from the upper-right. The strong field region is again positive, but the weak field regions appear to have reversed their polarities such that the left side is now negative and the right side is now positive. The old neutral line has disappeared and a new one has formed, this time at the leftmost  $V_0$  line. The magnetic associations of the two  $V_0$  lines are now switched compared to the previous view.

An important point is that the Doppler shift pattern remains unchanged relative to the strong and weak magnetic fields, but the magnetic polarity pattern is different depending on the view. Strong field regions remain redshifted and weak field regions remain blueshifted, but the weak field regions have variable polarity owing to the horizontal nature of the field. Such behavior is confirmed in observations of individual active regions rotating across the disk.



Note that the limb is in opposite directions for the two views of Figure 5; in the first view the limb is to the right, and in the second view the limb is to the left. As a consequence of this asymmetry, the  $V_0$  line that is observed at a neutral line always has a limbward blueshift. Similarly, the  $V_0$  line that is observed in a unipolar region always has a limbward redshift. These are exactly the trends that are so dominate in Table II.

Another result of Table II--that  $V_0$  lines associated with neutral lines and unipolar regions are equally common--is also predicted naturally by the model. Every  $V_0$  line that is at one time associated with a neutral line must at some other time be associated with a unipolar region (assuming that the feature is long-lived, which Paper I indicates is likely).

In short, the active region model proposed in Paper I is able to explain all of the important observational results of Table II and all but the weak field region results of Table III. (It is not inconsistent with the weak field results, but simply does not apply.) We have been unable to find an alternate model for which this is true. Some models can explain the results of Table II (e.g., Athay *et al.*, 1983b; Athay and Klimchuk, 1987), but they are inconsistent with the magnetic boundary and strong field region results of Table III. The current study therefore provides additional corroborative evidence for the model of Paper I. In addition, because this study includes many more active regions than were examined Paper I, it greatly expands the model's generality.

The model, as presented, is not concerned with the subset of  $V_0$  lines that are observed in the weak field areas outside of active regions, however. Those  $V_0$  lines make up a majority of the weak field region

associations in Table III and they account for many of the unipolar region and neutral line associations in Table II. It is possible to modify the model to explain these features, as well, if we simply assume that the vertical fields are weaker than 100 G. Some of the flux from active regions must be connected to the quiet Sun, and one might imagine that the field strength is reduced at those location. It is not obvious how the magnetic network fits into this picture, but we note that weak field  $V_0$  lines are often observed close to the limb, where considerable spatial averaging takes place.

Because of the fewer observational constraints (no magnetic boundary results to explain), this modified model is not unique in weak field regions. Athay and Klimchuk (1987) have proposed a different model that can account for the  $V_0$  line observations in these regions (see also Athay, 1987). In that model *all* of the field lines have an elliptical shape, and the ratio of the horizontal axis of the ellipse to the vertical axis is less than 2 (i.e., the loops are well-rounded). The authors assume a downflow in both sides of the loops, and they invoke projection effects to explain the observed correlations between Doppler shift and magnetic field polarity. Such effects result from the height difference between the photosphere and transition region and may cause vertically aligned features to appear displaced by as much as 4" near the limb. It is likely that these effects are responsible for many of the ambiguous associations that are listed in Tables II and III.

Unlike Athay and Klimchuk (1987), we do not specify a flow in our model *a priori*. We simply relate the topology of the magnetic field to the observed Doppler shift patterns, whatever their origin. It is important to remember that the observed Doppler shifts discussed throughout this

and related papers are relative to a rather arbitrary zero point. The usual practice is to normalize Dopplergrams such that the average Doppler shift vanishes, yet existing measurements of *absolute* Doppler shifts suggest that the average Doppler shift in a properly calibrated Dopplergram should be 4-11 km s<sup>-1</sup> to the red (Klimchuk, 1986 and references therein). Thus, the substantial blueshifts that appear in uncalibrated Dopplergrams may actually correspond to Doppler shifts of very small magnitude, possibly to the blue and possibly to the red.

This zero point uncertainty helps to explain how the regions of horizontal field and, presumably, horizontal flow in Figure 5 can be "blueshifted" for both views, an apparent contradiction. Properly calibrated Dopplergrams might show small blueshifts for one view and small redshifts for the other view, which is consistent with a slow horizontal flow. Our model, in fact, predicts that this should be the case.

One consequence of this interpretation is that the absolute redshifts which are implied for vertical field regions are independent of the disk location where they are observed. A vertical downflow would produce a distinctive center-to-limb variation, on the other hand. This apparent dilemma deserves much further discussion, which we postpone for the third paper of this series.

The author wishes to thank R. Grant Athay and Thomas E. Holzer for helpful suggestions during the course of this work. Dr. Athay also provided useful comments on the manuscript. A portion of this work was supported by the Naval Research Laboratory while the author was a National Research Council Cooperative Research Associate and also by NASA Grant NGL 05-020-272, Office of Naval Research Contract

N00014-85-K-001, and as part of the Solar-A collaboration under NASA Contract NAS8-37334 with Lockheed Palo Alto Research Laboratories.

TABLE I  
Magnetic Associations of  $V_0$  Lines

Active Region No.	$V_0$ Line No.	Full Disk Mag. Classification*	Extracted Image Classification*
2588	1	Neutral Line	Boundary
	2	Unipolar	Boundary
2684	1	Neutral Line	Ambiguous
	2	Unipolar	Ambiguous
	3	Sunspot	Sunspot
	4	Ambiguous	Weak Field
2469	1	Neutral Line	Weak Field
	2	Ambiguous	Weak Field
	3	Neutral Line	Ambiguous
	4	Sunspot	Sunspot
	5	Unipolar	Ambiguous
	6	Unipolar	Weak Field
	7	Neutral Line	Str. Field NL

\*key: Unipolar -- Unipolar Region  
 Boundary -- Magnetic Boundary  
 Weak Field -- Weak Field Region  
 Str. Field NL -- Strong Field Neutral Line

TABLE II

Magnetic Associations: Full Disk Magnetograms  
(number of occurrences)

Limbward Doppler Shift	Unipolar Region	Neutral Line	Sunspot	Ambiguous
Red	33	3	4	35
Blue	4	41	10	28
Neither	5	4	0	14
Total	42	48	14	77

TABLE III  
Magnetic Associations: Extracted Images  
(number of occurrences)

Limeward Doppler Shift	Strong Field Region	Weak Field Region	Magnetic Boundary	Strong Field Neutral Line	Sunspot	Ambiguous
Red	1	13	8	0	2	23
Blue	0	6	10	1	10	22
Neither	0	0	3	0	0	4
Total	1	19	21	1	12	49

## References

Athay, R. G.: 1987, *Nature* **327**, 685.

Athay, R. G., Gurman, J. B., Henze, W., and Shine, R. A.: 1982, *Astrophys. J.* **261**, 684.

Athay, R. G., Gurman, J. B., Henze, W., and Shine, R. A.: 1983a, *Astrophys. J.* **265**, 519.

Athay, R. G., Gurman, J. B., and Henze, W.: 1983b, *Astrophys. J.* **269**, 706.

Athay, R. G., and Klimchuk, J. A.: 1987, *Astrophys. J.* **318**, 437.

Howard, R. and Harvey, J.: 1970, *Solar Phys.* **12**, 23.

Jones, H. P., and Giovanelli, R. G.: 1982, *Solar Phys.* **79**, 247.

Klimchuk, J. A.: 1986, in A. I. Poland (ed.), *Coronal and Prominence Plasmas*, NASA CP-2442, p. 183.

Klimchuk, J. A.: 1987, *Astrophys. J.* **323**, 368 (Paper I).

Malherbe, J. M., Schmieder, B., Simon, G., Mein, P., and Tandberg-Hanssen, E.: 1987, *Solar Phys.* **112**, 233.

### Figure Captions

Fig. 1. Four images of Active Region #2588, observed toward the west limb: (upper-left) C IV Dopplergram; (upper-right) linear magnetogram plot,  $\pm 100$  G dynamic range; (lower-right)  $\pm 100$  G contour plot, contours filled-in; (lower-left) Fe I wing spectroheliogram. Dark shades correspond to relative blueshifts, negative line-of-sight magnetic fields, and low intensities in the respective images. The Dopplergram has been rotated to the time of the other observations. Selected  $V_0$  lines have been marked on the Dopplergram and transferred to the other images for spatial reference. Numbers refer to Table I.

Fig. 2. As in Fig. 1, but for Active Region #2684 observed near the west limb. Only those portions of the  $V_0$  lines that are assigned a magnetic association are shown in the bottom two images.

Fig. 3. As in Fig. 1, but for Active Region #2469 observed near the east limb. Only those portions of the  $V_0$  lines that are assigned a magnetic association are shown in the bottom two images.

Fig. 4. Schematic drawing showing the relationships between the various magnetic features of the two different classification systems. Field strength is indicated by the boldness of the plus and minus polarity symbols.

Fig. 5. Schematic drawing of the proposed magnetic topology in relation to the observed Doppler shift patterns. Arrows indicate the direction of



the magnetic field in the upper photosphere and should *not* be confused with flow vectors. Two lines-of-sight corresponding to observations made in the eastern and western hemispheres are indicated. "R" and "B" designations refer the redshifts that are seen in vertical (strong) field regions and blueshifts that are seen in horizontal (weak) field regions. Pluses and minuses refer to the line-of-sight polarity of the field.

AR 2588 2 AUG 1980

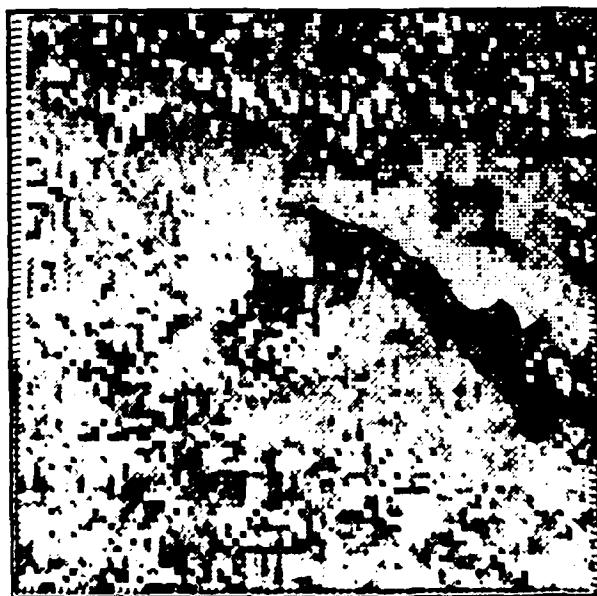
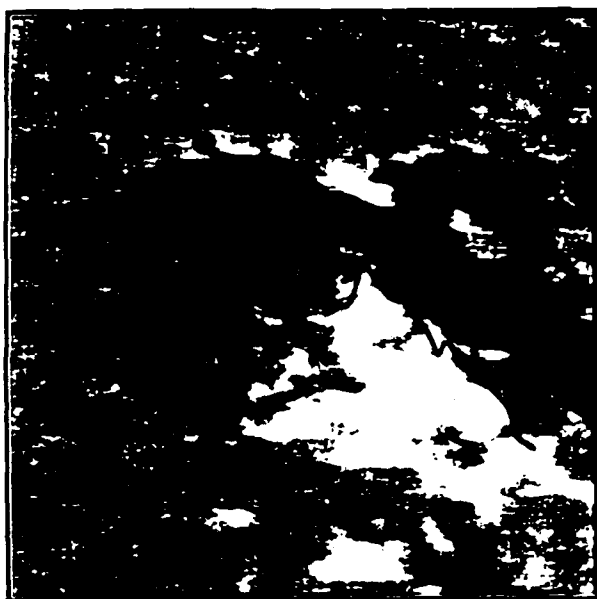


Fig. 1

AR 2684 26 SEP 1980

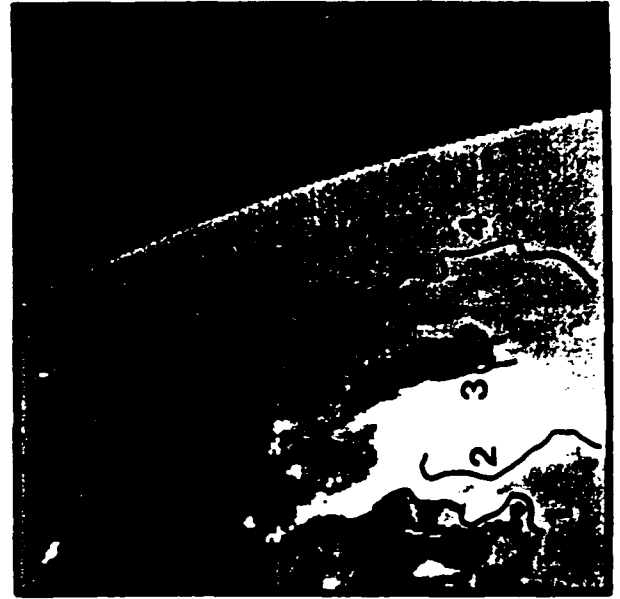
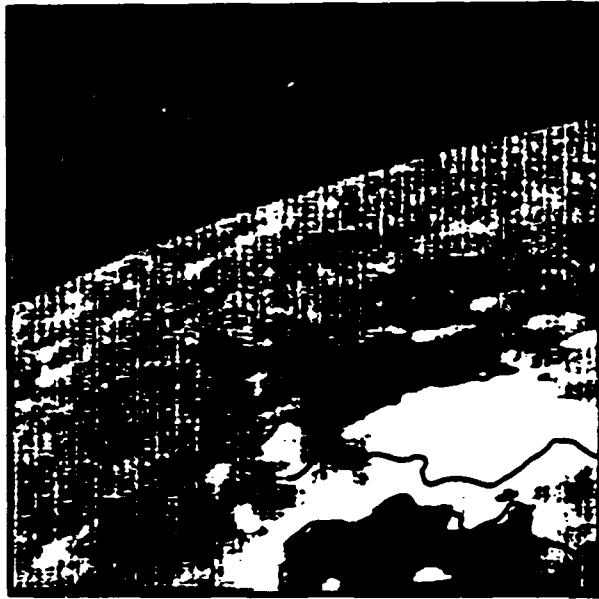


Fig. 2

AR 2469 21 MAY 1980

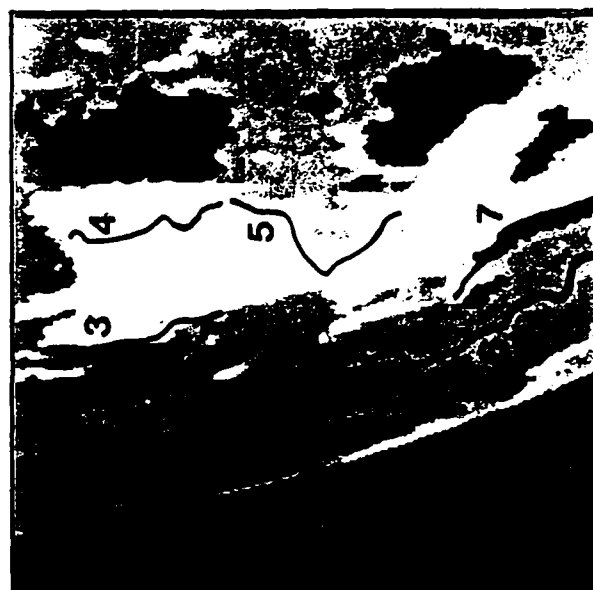


Fig. 3

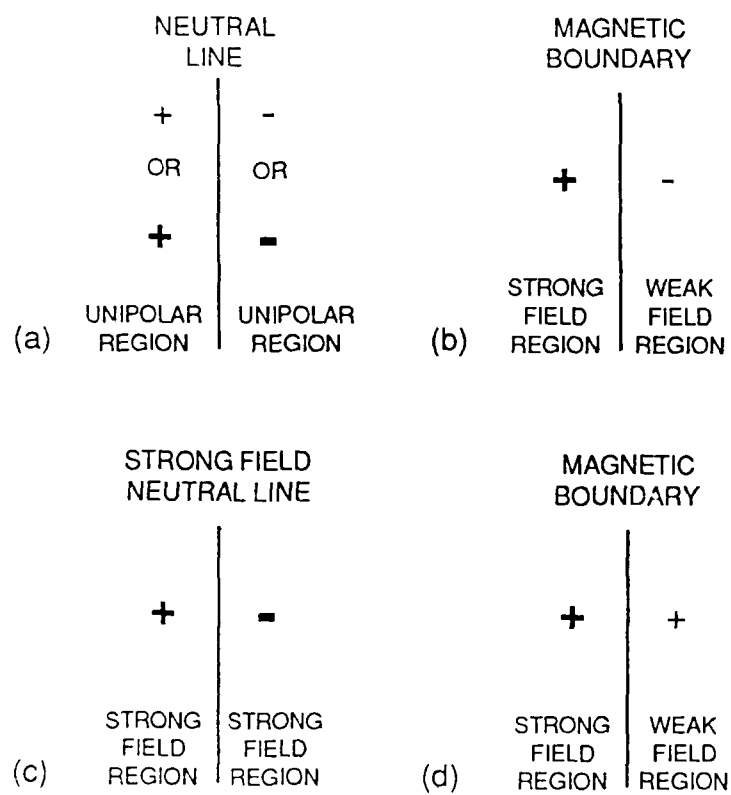


Figure 4

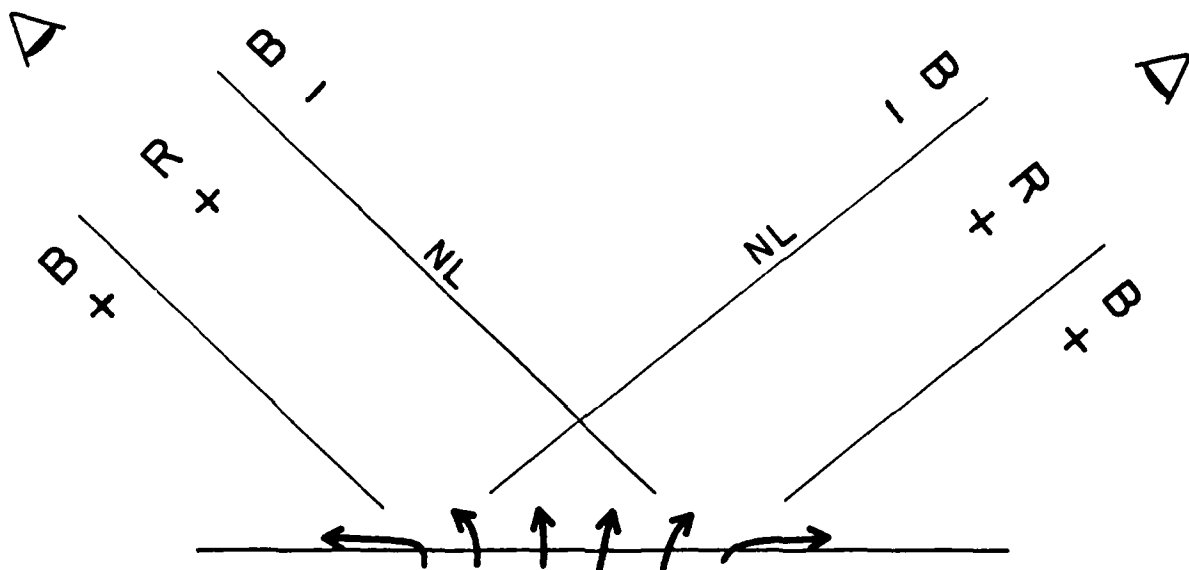


Figure 5

**Article Title:**

"Magnetic Properties of C IV Doppler Shift Patterns"

**Author:**

James A. Klimchuk

**Affiliation:**

High Altitude Observatory,  
National Center for Atmospheric Research

**Postal Address:**

Center for Space Science and Astrophysics  
Stanford University, ERL 300  
Stanford, CA 94305